



Vanadium Distribution in Four-Component Mo-V-Te-Nb Mixed-Oxide Catalysts from First Principles: How to Explore the Numerous Configurations?*

Gang Fu, Xin Xu, and Philippe Sautet*

Selective oxidation is a major catalytic process in the chemical industry for the synthesis of value-added chemicals, such as alcohols, esters, ethers, and acids.^[1] The aim to replace olefins with cheaper alkanes as feed gases drives the development of new catalysts that should activate alkane C–H bonds and show high selectivity for the formation of the target molecules. For the selective oxidation of propane, a multicomponent Mo-V-Te-Nb oxide has shown great promise.^[2] This complex system exists in two phases referred to as M1 and M2, whereby orthorhombic M1 is thought to be responsible for propane C–H activation and for the formation of acrylic acid.^[2–5]

The structure of the M1 phase is characterized by a network of MO₆ octahedra (M = Mo, V) arranged in three types of rings: pentagonal, hexagonal, and heptagonal (Figure 1).^[6–9] The nonequivalent metal sites are labeled S1–S13. The pentagonal ring is centered on a pyramidal biprismatic unit (S9) containing one Nb atom and surrounded by five octahedra (S5, S6, S8, S10, and S11, referred to as ring sites, light gray). These pentagonal units are linked together through corner-sharing octahedra (S1, S2, S3, S4, and S7, referred to as link sites, dark gray). This arrangement generates open hexagonal and heptagonal channels in which TeO units may be positioned (S12 and S13). This stacked 2D array of nondensely packed metal–oxygen polyhedra is representative of the three-dimensional structure of several multicomponent metal oxides.

Hence, the key question is to determine the distribution of V and Mo atoms at the various octahedral sites.^[6–9] Rietveld refinement showed that although sites S1–S11 are always fully occupied, the distribution of Mo or V at S1–S7 and S11 is fractional (V occupation ranges from 0 to 60%; see Table 1S

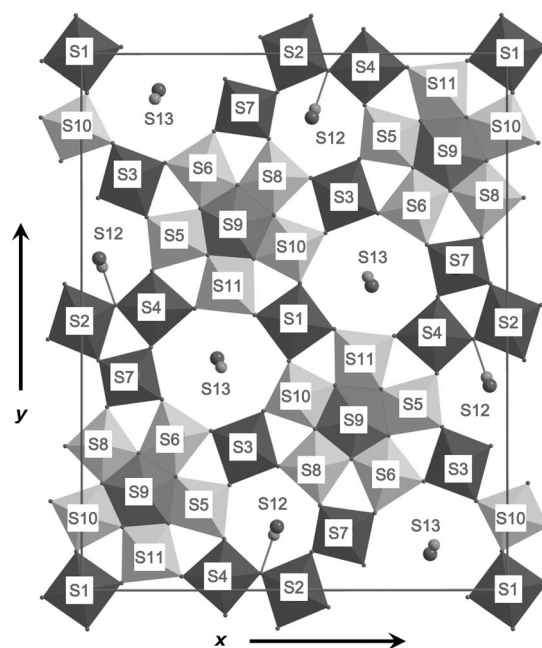


Figure 1. Structure of the M1 phase of MoVTeNbO₄ (orthorhombic) as viewed along the (001) basal plane. The various sites for Mo, V, and Nb atoms are shown as oxygen polyhedra: pentagonal (S9) and octahedral ring sites (light gray), and octahedral link sites (dark gray). Light/dark balls represent the Te/O atoms in the channels.

in the Supporting Information). In the selective oxidation of propane, V and Mo do not have the same role. It is therefore of utmost importance to understand how these two elements are positioned as well as the nature of the most frequent clusters in the structure. However, the very large number of coordinates in the unit cell (up to 200 unequivalent coordinates) hinders compositional and structural determination.^[6–9] For example, the V occupation determined by different refinements can vary by up to 40%. The difficulty in experimental structure determination is also illustrated by the significant differences in M–O bond distances in Mo/V octahedra (they can differ by up to 0.24 Å; see Table 2S).^[6–9] This situation is not unique to the M1 phase, and several mixed oxides show a similar fractional occupation/distribution of sites that obscures the understanding of their properties and makes their atomistic simulation very challenging. The study of such complex oxides with partial occupations is hence an important challenge in the field of inorganic materials.^[10]

Explicit atomistic modeling of these systems requires integer occupations of the sites. Therefore, it is necessary in

[*] G. Fu, P. Sautet
Université de Lyon, CNRS, and Ecole Normale Supérieure de Lyon
46 Allée d'Italie, 69364 Lyon Cedex 07 (France)
E-mail: philippe.sautet@ens-lyon.fr

G. Fu
State Key Laboratory for Physical Chemistry of Solid Surfaces and
College of Chemistry and Chemical Engineering
Xiamen University (P.R. China)

X. Xu
Department of Chemistry, Fudan University (P.R. China)

[**] We thank the PSMN at the ENS Lyon and IDRIS-CNRS for computational resources and the NSFC (21133004, 20973139), the NSF of Fujian Province (2009J05035), and the Fundamental Research Funds of Central Universities for financial support.

Supporting information for this article is available on the WWW under <http://dx.doi.org/10.1002/anie.201207638>.

principle to use large supercells and to explore a huge number of configurations. A pioneering approach was developed by Goddard et al., who used a $2 \times 2 \times 2$ super cell (1280 atoms) and empirical reactive force fields.^[11] The billions of possible configurations of the metal atoms are probed by a Monte Carlo (MC) reaction-dynamics approach, which combines molecular dynamics, geometry optimization (OPT), and MC jumps. Force-field methods are able to provide reasonable geometries in many cases; however, they do not explicitly take into account the electronic structure of the considered metal. They are suitable for the study of simple oxides but have limitations in the case of mixed-valence systems, in which a given metal can appear with different electronic occupations. In Mo-V-Nb-Te, V can be present in +IV and +V oxidation states, and Mo in +V and +VI oxidation states. The electronic properties of the V and Mo atoms in the structure depend on their location. Thus, the M1 phase (like other mixed oxides) is not only structurally but also electronically complex. Calculations based on first principles can describe the electronic structure; however, the exploration of a large number of configurations for a complex multicomponent oxide remains a challenge.

Herein, we present an approach for the first-principles evaluation of the distribution of metal atoms in the M1 structure. A large number of local configurations were evaluated from periodic DFT calculations of a single unit cell of the M1 phase (160 atoms). In a second step, the optimal distribution was determined on the basis of Boltzmann statistics. It was assumed that all Te atoms are located in the hexagonal channel and that the configuration space for the V atoms is limited to the linking sites (S1, S2, S3, S4, S7), whereas Mo always occupies other octahedral sites. There are 16 linking octahedra in the unit cell, five of which are crystallographically distinct. The total number of possible configurations is 120, 560, 1820, and 4368 for two, three, four, and five V atoms in the unit cell, respectively. For the chemically realistic possibility that six V atoms are present in the unit cell, the number reaches 8008 (or 2059 symmetry-independent configurations). If all configurations were fully optimized with DFT, the computational effort would be extremely large. We present herein a constructive model that can accelerate the simulation and be used to estimate the V occupancy by exploring the whole configuration space.

We begin with the case of a single V substitution, for which only five unique configurations (S1, S2, S3, S4, and S7) need to be considered. The relative energies were calculated to be 0.38, 0.00, 0.21, 0.30, and 0.21 eV, respectively. The stability order is hence $S2 > S3 \approx S7 > S4 > S1$. It was found experimentally that V-atom occupancies in the S2, S3, and S7 sites are relatively high, whereas S4 sites are mainly occupied by Mo atoms (see Table 1S). Pyrz et al.^[12] speculated that S4 would have a similar occupancy to that of S7, as these two sites have the same coordination environment. However, the DFT results showed that V-atom substitution at S4 sites is less favorable than at S7 by 0.09 eV and thus implied a preference for S7.

Unfortunately, a full OPT for the 160-atom unit cell requires about 2 days on a quad-core PC server, so that a complete exploration of all configurations for a high V

content would be a highly CPU intensive task. In fact, configuration statistics only require the relative energies of different configurations. To simplify the task, we considered that the substitution of Mo by V would not lead to a strong structural relaxation and that the relative energies determined by single-point (SP) calculations for the nonrelaxed structure could reproduce well those derived by OPT. To decrease further the CPU time, we used less accurate but reasonable parameters in the SP calculations (see the Supporting Information for details). The optimized M1 model with only Mo atoms and no V substitution was used as the initial structure. V atoms were then placed at positions originally occupied by Mo, and the corresponding V=O bond was shortened to 1.63 Å, a usual value for vanadium oxo compounds.^[13] For single V substitution, the relative energies determined by this simple nonrelaxed SP approach showed a mean absolute deviation (MAD) lower than 0.01 eV from the values determined by OPT, which validated the approach. The computational cost for an SP task is only 1 h, which corresponds to a 98 % reduction in CPU time relative to that required for OPT. Hence, the SP approach allows the exploration of thousands of configurations.

Nevertheless, it was first necessary to check the accuracy of these SP energies for multiple vanadium-atom substitutions. For the substitution of two V atoms, the correlation between the OPT and SP energies was still very good, with an R^2 value of 0.95 and the slope of the regression close to 1 (0.95). Thus, the relative energies determined from the OPT or SP calculations were very similar (see Figure 1S and 2S for details). For three points, however, the SP energy was higher than the regression line by more than 0.05 eV; these configurations involved a nearest-neighbor V–V pair. All of these results indicate that SP calculations can give accurate relative energies when the V sites are not nearest neighbors in the structure; however, the total energies of configurations with adjacent V sites are overestimated. Undoubtedly, this situation would become more complicated with a further increase in the vanadium content. Indeed, our calculations show that the R^2 value gradually deteriorates from 0.62 for four V atoms, to 0.40 for five V atoms, to 0.28 for six V atoms (the case of six vanadium atoms is shown in Figure 2A). These poor correlations indicate that SP energies cannot be used as a good estimate of the relative energies for multiple V substitutions.

The main difficulty is the excessive destabilization between neighboring V atoms in the structure in the absence of relaxation. In the following, we propose a modified scheme for the correction of these excessive repulsions. From the singly substituted configurations, one can calculate the V-substitution energy for each site S_i :

$$\Delta E_{\text{sub}}(S_i) = E(S_i) - E(\text{Mo}) \quad (1)$$

In Equation (1), $E(S_i)$ stands for the total energy of a single vanadium-atom substitution at a given site S_i , whereas $E(\text{Mo})$ is the energy for the M1 model with full Mo occupation. A zero-order approximation for the energy of configurations with n V atoms can be constructed by summing up the individual substitution energies:

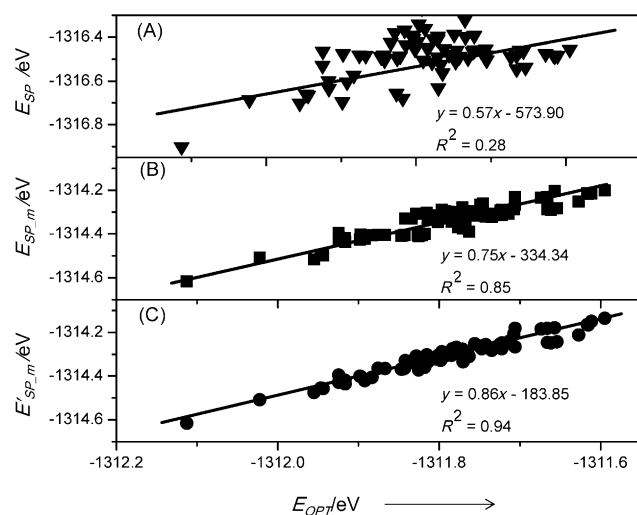


Figure 2. Correlation between optimized energies (E_{OPT}) and A) single-point energies (E_{SP}), B) modified SP energies (E_{SP_m}), and C) modified SP energies including next-nearest-neighbor corrections (E'_{SP_m}). Six V atoms were put in the unit cell.

$$E_0(nV) = E(\text{Mo}) + \sum_{i=1}^n \Delta E_{\text{sub}}(\text{Si}) \quad (2)$$

Clearly, this approximation always underestimates the total energy for configurations with an adjacent V–V pair, since V–V repulsions are neglected. A new energy descriptor, E_{SP_m} , can be obtained by mixing with identical weights E_{SP} (which overestimates V–V interactions) and $E_0(nV)$ (which underestimates V–V interactions):

$$E_{\text{SP}_m} = \frac{1}{2} (E_{\text{SP}} + E_0(nV)) \quad (3)$$

E_{SP_m} energies are plotted against OPT energies in Figure 2B (see also Figure 3S). For the case of two V atoms (see Figure 3SA), there is a perfect linear relationship ($R^2 = 0.99$), which shows that energy overestimation from SP calculations can be compensated well by mixing with $E_0(nV)$. For four and five V atoms, the energy deviations from a linear fit are strongly narrowed, and the R^2 values (0.94 and 0.85, respectively) are significantly improved (see Figure 3SB,C). For six V-atom substitutions, the R^2 value was calculated to be 0.85, which is far higher than that found for the direct SP calculation ($R^2 = 0.28$; Figure 2A,B). Thus, SP_m energies correlate well with OPT energies and can be used as predictors.

Figure 3 illustrates why the modified SP method works. The x axis indicates the strength of the V–V interaction, and the y axis the calculated total energy. The left-hand side corresponds to a noninteracting system, in which the V–V interaction is ignored ($E_0(nV)$), whereas the right-hand side corresponds to a constrained system without any structural relaxation (E_{SP}). The total energy of an optimized structure (E_{OPT}) is located in between these two limiting values, $E_0(nV)$ and E_{SP} , such that the half-and-half mixture of energies given by E_{SP_m} becomes a good approximation for the OPT energy. Mixing of the two energies in equal proportions is arbitrary, and the optimum weights could be system-dependent.

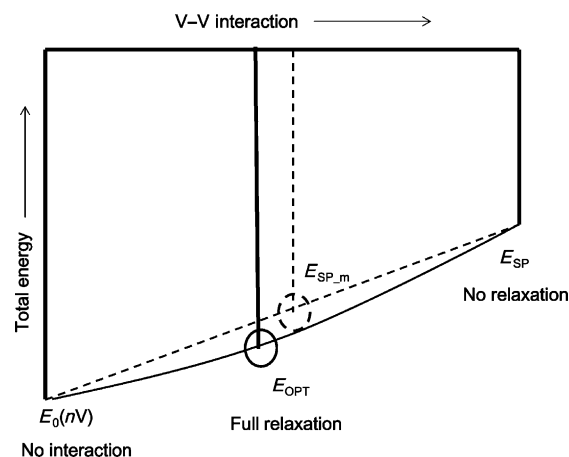


Figure 3. Relationship between the different energetic scenarios.

For better accuracy, one can further consider the next-nearest-neighbor V–V interactions (see Figure 4S). When such a pair is found in a configuration, an additional correction is simply added to E_{SP_m} to give E'_{SP_m} . This correction improves the correlation significantly ($R^2 > 0.94$ in all cases; Figure 2C; see also Figure 5S). Although such energy corrections are very small (0.02–0.04 eV), they can accumulate in the cases of four, five, and six V-atom substitutions and are hence significant in the energy estimation.

In going from a calculation of E_{SP} to a calculation of E'_{SP_m} , there is no additional computational cost. Thus, by means of the modified SP method, we can quickly survey the complete configuration space and determine the most stable configurations from thousands of possibilities. The final set of configurations to be optimized for the correlation in Figure 2 was established by first calculating E'_{SP_m} for all configurations and then selecting all those configurations with an energy up to 0.4 eV above that of the most stable configuration. In this way, we can obtain optimized energies (E_{OPT}) for a limited set of configurations (<100) or estimated energies (E'_{SP_m}) spanning the complete configuration space (ca. 2000).

The average over the configuration set for any property ($\langle X \rangle$), such as V occupancy and V–V pair probability, can be obtained by Equation (4):

$$\langle X \rangle = \sum_{m=1}^N (P_m X_m) \quad (4)$$

In this equation, X_m stands for the calculated value of X for a configuration m , and P_m is the probability of this configuration, which is energy-dependent:^[14]

$$P_m = \frac{1}{Z} \exp\left(-\frac{\Delta E_m}{kT}\right) \quad (5)$$

Z denotes the normalization factor:

$$Z = \sum_{m=1}^N \exp\left(-\frac{\Delta E_m}{kT}\right) \quad (6)$$

The most significant descriptor is the partial occupation of sites in the M1 structure.^[6–9] For MoVTeNbO_x, determination of the location of V atoms is a key prerequisite for understanding the active centers as well as the detailed molecular mechanism of selective alkane oxidation.^[2,5–7] For a given site, experiments found different V/Mo ratios over time (see Table 1S). For example, the partial occupancy of V in the S2 site can vary from 0.4 to 0.8. Additionally, recent results suggested that the S4 site, which was believed to be 100% Mo in earlier studies, has a partial V occupancy of 0.1–0.2.^[8,9] Such differences might be attributed to the complex refinement procedure and to different total V content in the samples.

The partial occupancy for the five most important sites is shown graphically in Figure 4A as a function of the number of V atoms in the unit cell. As expected, the partial occupancy of a site increases with the total V content, but the extent and timing of the increase depends on the particular site. The S2 site shows a fast increase for low V contents (from one to two V atoms), whereas the occupation of other sites starts later. S3, for example, shows a large occupation only when four V atoms are substituted. At the same V content, S7 and to a smaller extent S4 and S1 also start to be occupied. Calculations hence clearly show that S2 is occupied first and that other sites are only occupied when four or more vanadium atoms are present in the unit cell. This behavior correlates well with the fact that a minimum content of V atoms (at least four) must be reached for the onset of catalytic activity.^[4] We can therefore conclude that S2 is not the active site. Experimental data correspond to the presence of 4.8–6.8

V atoms in one unit cell. The distribution, with high occupation of S2 and S3, lower occupation of S7, and very low occupation of S4, agrees well with the theoretical results. However, there is a significant deviation for S1, the V occupation of which is relatively high according to the experimental data (20–54%) and lower (maximum 10%) according to our calculations. A large number of configurations have a significant weight: the 10 most probable configurations account for only about 50% of the total probability (see Figure 6S). It is hence difficult to propose an explicit atomistic model of the M1 phase. In configurations with the highest probability, V atoms occupy S2, S3, and S7. Detailed analysis of the electronic distribution and oxidation number of the metal cations is of great chemical importance but requires a more sophisticated approach than the use of the GGA functionals employed in this study. >

Grasselli et al. suggested that the selective oxidation of propane to acrylic acid or acrylonitrile involves a complex sequence of transformations that requires more than a single active center.^[2] Owing to the partial occupancy in MoVTeNbO_x, understanding the probability of a given specific distribution of atoms in one unit cell (and not only in an averaged manner over the complete crystal) becomes an important issue. We therefore introduce a new descriptor, the pair probability $P_2(S_i, S_j)$ of finding two sites occupied by a given element in the same cell. This pair probability cannot be deduced from experiment, which only provides average occupancy. For simplicity, we focus on the pair probability of finding two V atoms in place of Mo atoms at two sites. On the basis of a mean-field approximation, the average pair probability $P_2(S_i, S_j)$ can be written as:

$$P_2(S_i, S_j) = P(S_i)P(S_j) \quad (7)$$

In Equation (7), $P(S_i)$ and $P(S_j)$ are the occupation probabilities for sites S_i and S_j , respectively. Theoretically, the difference between $P_2(S_i, S_j)$, calculated by using Equation (4), and $P_2(S_i, S_j)$ is associated to correlation effects. We define the relative correlation probability $P_{\text{corr}}(S_i, S_j)$ as:

$$P_{\text{corr}}(S_i, S_j) = \frac{\langle P_2(S_i, S_j) \rangle - P_2(S_i, S_j)}{P_2(S_i, S_j)} \quad (8)$$

A 16×16 matrix can be established (Figure 4B) in which gray tones show the degree of correlation (equivalent V sites need to be distinguished in this case, since they form distinct pairs with other sites). Interestingly, all relative correlation probabilities were negative, and the values were most negative in the case of nearest (S4–S7) and next-nearest V–V interactions (S1–S3, S3–S7). Pair probabilities for such pairs are considerably lower than those obtained from the mean-field approximation: by 32% (S1–S3, S3–S7) or even 74% (S4–S7). This finding indicates that V atoms are not arranged independently of one another in Mo–V–Te–Nb oxides and that correlations need to be taken into account to describe multiply substituted unit cells.

A last important aspect is the geometry of the substituted sites. For Rietveld refinement, about 200 parameters should be resolved, which leads to significant structural uncer-

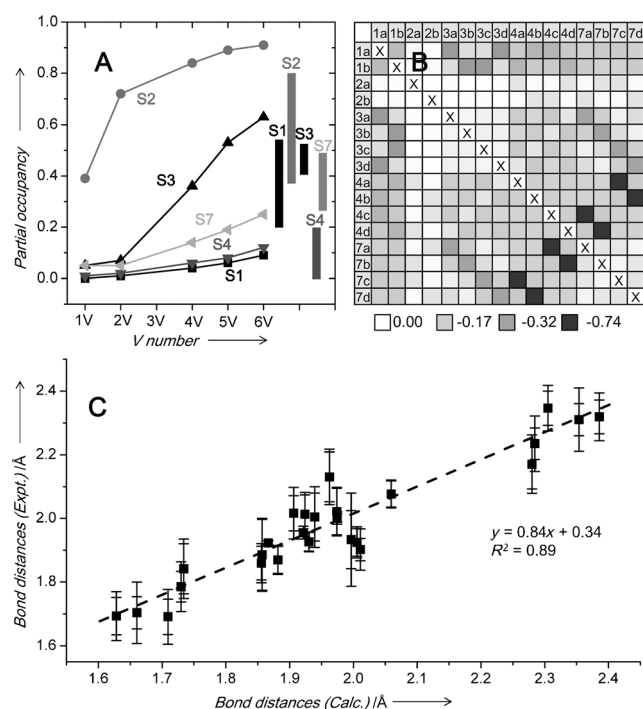


Figure 4. A) Calculated partial V occupancies in linking S_i sites as a function of V content. The experimental ranges found for 4.8–6.8 V atoms are shown as vertical bars. B) V–V pair relative correlation probabilities, $P_{\text{corr}}(S_i, S_j)$, among all linking sites. C) Average M–O bond distances from different experiments versus calculated bond distances.

tainty.^[6–9] In fact, the obtained element distribution also depends critically on the determined structure of the oxide, especially for the V/Mo mixed sites. The average M–O bond distances can be obtained from the set of optimized configurations.

Figure 4C displays the theoretical average M–O bond distances for six V-atom substitutions versus the experimental values. The average M–O distances correlate well with the mean values derived from different experimental data ($R^2 = 0.89$), but significant deviations occur. When the deviation between experiments is relatively narrow, that is, there is minor structural uncertainty, good agreement between experiment and theory can be seen. For example, the maximum deviation between the four experiments for S7–O(–S4) is only 0.09 Å, and the average values deduced from theory and experiment are close (1.881 versus 1.870 Å). However, the slope of the regression is 0.83, which indicates a systematic error between experimental and theoretical estimations. The experimental determination of these complex structures is very challenging, and first-principles calculations could propose geometric parameters to facilitate the refinement.

In summary, we have developed a cost-efficient DFT-based method that demands only 1–2% of the CPU time required for full optimization. By this method, thousands of configurations can be simulated and average properties can be evaluated by using Boltzmann weighting factors. These calculations showed that V-atom occupancies of particular sites follow the order $S2 > S3 > S7 > S4 \approx S1$ in line with experimental observations. S2 is occupied first, and other sites are occupied when there are four or more V atoms in the unit cell. These results provide insight on the observed activity upon increases in the V content. The arrangement of V–V pairs shows significant negative correlation effects, which result in a decrease in the pair probabilities relative to those found by an independent particle approximation. This difference in the pair probabilities has important consequences in terms of the nature of the multimetal active sites and potential reaction mechanisms. Moreover, the good correlation of the calculated average M–O bond distances with the mean

experimental values highlights the power of first-principles simulation. Finally, we expect that such an approach will be applied to related systems of importance in catalysis, such as zeolites, other mixed oxides, or alloys.

Received: September 20, 2012

Published online: November 21, 2012

Keywords: configuration statistics · DFT calculations · heterogeneous catalysis · multicomponent metal oxides · selective oxidation

- [1] G. Centi, F. Cavani, F. Trifiró, *Selective Oxidation by Heterogeneous Catalysis*, Kluwer Academic/Plenum, New York, **2001**.
- [2] R. K. Grasselli, C. G. Lugmair, A. F. Volpe, Jr., *Top. Catal.* **2011**, *54*, 595–604.
- [3] V. V. Guliyants, R. Bhandari, B. Swaminathan, H. H. Brongersma, A. Knoester, A. M. Gaffney, S. Han, *J. Phys. Chem. B* **2005**, *109*, 24046–24055.
- [4] F. N. Naraschewski, A. Jentys, J. A. Lercher, *Top. Catal.* **2011**, *54*, 639–649.
- [5] R. Schlögl, *Top. Catal.* **2011**, *54*, 627–638.
- [6] P. DeSanto, Jr., D. J. Buttrey, R. K. Grasselli, C. G. Lugmair, A. F. Volpe, B. H. Toby, T. Vogt, *Top. Catal.* **2003**, *23*, 23–38.
- [7] P. DeSanto, D. J. Buttrey, R. K. Grasselli, C. G. Lugmair, A. F. Volpe, B. H. Toby, T. Vogt, *Z. Kristallogr.* **2004**, *219*, 152–165.
- [8] H. Murayama, D. Vitry, W. Ueda, G. Fuchs, M. Anne, J. L. Dubois, *Appl. Catal. A* **2007**, *318*, 137–142.
- [9] X. Li, D. J. Buttrey, D. A. Blom, T. Vogt, *Top. Catal.* **2011**, *54*, 614–626.
- [10] K. Chenoweth, A. C. T. van Duin, W. A. Goddard III, *Angew. Chem.* **2009**, *121*, 7766–7770; *Angew. Chem. Int. Ed.* **2009**, *48*, 7630–7634.
- [11] W. A. Goddard III, J. E. Mueller, K. Chenoweth, A. C. T. van Duin, *Catal. Today* **2010**, *157*, 71–76.
- [12] W. D. Pyrz, D. A. Blom, T. Vogt, D. J. Buttrey, *Angew. Chem.* **2008**, *120*, 2830–2833; *Angew. Chem. Int. Ed.* **2008**, *47*, 2788–2791.
- [13] M. Schindler, F. C. Hawthorne, W. H. Baur, *Chem. Mater.* **2000**, *12*, 1248–1259.
- [14] R. Grau-Crespo, S. Hamad, C. R. A. Catlow, N. H. de Leeuw, *J. Phys. Condens. Matter* **2007**, *19*, 256201.